Optimization and performance characteristics of servo-piston hydraulic control rod drive mechanism

YU Mingrui[1] , HAN Weishi[2]， and WANG Ge[3]

1. *Fundamental Science on Nuclear Safety and Simulation Technology Laboratory, Harbin Engineering University, 145-1 Nantong Street, Nangang District, Harbin,150001, Heilongjiang, P.R China(yumingrui2010@sina.com)*

2. *Fundamental Science on Nuclear Safety and Simulation Technology Laboratory, Harbin Engineering University, 145-1 Nantong Street, Nangang District, Harbin,150001, Heilongjiang, P.R China(hanws2007@163.com)*

3.Beijing Institute of Control Engineering,16 Nansan Street, Haidian District, Beijing ,102413, P.R China(wangge522@sina.com)

Abstract: This paper introduces the structure and working principles of the servo-piston hydraulic control rod drive mechanism(SHCM), which can be moved continuously and has self-lock capacity. The steady state characteristics of SHCM are simulated using FLUENT codes. Based on comparison with the experimental results, the simulation is proven to be credible as a tool to describe the steady state characteristics. Finally, the influence of structural parameters is analyzed to obtain an optimal design. The experimental results indicate that the traction of the servo-tube is larger in the starting and braking stages. The resistance coefficient of SHCM increases gradually in the starting and lifting stage, and then tends to be stable. This coefficient has a maximum value while the inlet pressure is low. Performance norms of SHCM, such as the anti-disturbance ability and positioning accuracy, are tested, the anti-disturbance ability of the actuator is strong while the inlet pressure is fluctuating. The positioning accuracy is high regardless of the action process (lifting or not).

Keyword: control rod drive mechanism; hydraulic drive; internal; anti-disturbance

1 Introduction

The control rod drive mechanism (CRDM) is a crucial piece of safety equipment, taking on important functions such as reactor start-up, power adjustment and reactor shut-down. A large number of CRDMs have been designed for nuclear reactors, to ensure the reactor operates safely, with a variety of different drive power sources (electric, hydraulic, etc.) being used to accomplish the same function. The magnetic lift control rod drive mechanism is widely used in existing pressurized water reactor systems [1].

The hydraulic control rod drive mechanism includes the traditional and the new type mechanisms, which differ according to the drive energy and installation method. The hydrostatic drive control rod is used in the traditional mechanism, while the new mechanism uses a dynamic pressure transmission. Furthermore, the traditional mechanism is installed at the bottom of the reactor, and the new mechanism can be installed at either the bottom or top. There are two key types of new hydraulic control rod drive mechanisms, the hydraulic control rod driving system (HCRDS) and the servo-tube guided hydraulic control rod driving system (STCM). HCRDS is a stepper drive mechanism which was designed by Tsinghua University, and has been applied in a 5MW nuclear heating reactor[2]. STCM is a continuous hydraulic drive mechanism, which was designed by Harbin Engineering University with few electronic components in the system [3-4]. Furthermore, the continuous movement of the STCM benefits the reactor power distribution flattening and improving the burn-up level of the fuel element, however, its structure is complex and the transmission line is long[9].

The servo-piston hydraulic control rod drive mechanism (SHCM) is another new hydraulic drive

Received date: March 04, 2014
(Revised date: May 13, 2014)

system. SHCM drives the control rod with fluid dynamic pressure, and can be moved continuously. In addition, the internal structure of SHCM is different from STCM, although the work principle is the same. The piston in SHCM is not only the drive actuator, but also the positioner. There are few electronic components and control valves in the system, and the transmission line is short due to the special transmission method. Furthermore, the servo tube tractor can keep the control rod position when power is lost. No study has previously been completed on SHCM. We aim to test the feasibility of SHCM, identify and optimize the critical components of the system by the numerical simulation and experimental analysis. Deeper research on STCM will be summarized in a further study.

The remainder of this paper is organized as follows: the working principle of SHCM is presented in Section 2. Section 3 illustrates the experimental system, and then the results from both experiments and numerical analyses are presented in Section 4 and Section 5. Finally, Section 6 concludes the paper.

2 Servo-piston hydraulic control rod drive mechanism

SHCM is a kind of continuous drive system which is based on the dynamic pressure difference generated by the fluid passing through the drive mechanism. Figure 1 shows the structure of SHCM, which includes a hydraulic driving cylinder, piston, servo tube, transmission belt, servo tube tractor and hydraulic motor. SHCM uses the reactor coolant as the working medium, the working medium is pressurized by a pump and ejected into to a filter, which will remove any particles with diameter larger than 0.1 mm from coolant, before sending it to the drive mechanism (See Fig.2).

When the fluid flows through the variable throttle orifice, due to the throttling effect of the servo tube, it will produce a pressure difference which acts on the piston. The pressure difference is as follows:

$$\Delta P = P_1 - P_2 = \Delta p_g + \Delta p_c = \frac{\xi_g \rho_w Q_1^{\ 2}}{2A_g^{\ 2}} + \frac{\xi_c \rho_w Q_2^{\ 2}}{2A_f^{\ 2}} \qquad (1)$$

where $A_f = \pi D_N \delta$ (2)

The upward force from the pressure difference acting on the piston is as follows:

$$F = \Delta P \cdot S = P_1 \frac{\pi}{4}\left(D_1^2 - D_2^2\right) - P_2 \frac{\pi}{4}\left(D_2^2 - A_0\right) \qquad (3)$$

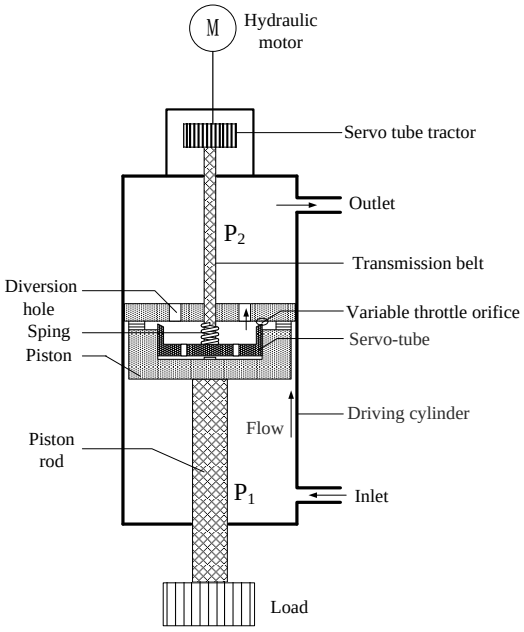

(a)Complete diagram

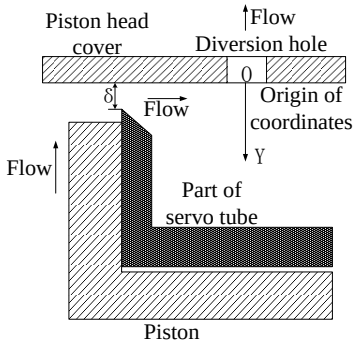

(b) Partial enlarged detail

Fig.1 Structure diagram of SHCM.

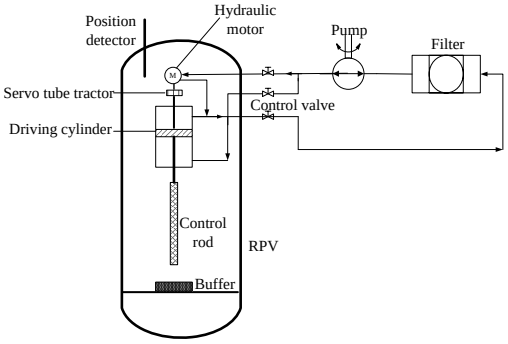

Fig.2 Schematic diagram of SHCM system.

Defining the flow from the entrance into the driving cylinder as the work flow. The friction between the piston and cylinder is ignored, therefore the force of the piston includes only gravity, buoyancy and the upward force. Defining the axial upward direction as positive, the piston movement equation is as follows:

$$F - G + F_{\Delta} = \Delta P \cdot A - m_c g + m_c g \frac{\rho_w}{\rho_a} = m_c \frac{d^2 x}{dt^2} \qquad (4)$$

With the proper pressure, the piston can keep balance in an equilibrium position, at this time, the gravity, the buoyancy and the upward force are balanced. *F* is controlled by changing the gap (δ) of the variable throttle orifice between the piston and the servo tube. When the servo tube is lifted by the tractor winding the transmission belt, the δ reduces and the pressure difference increases because of the stronger throttling action, thus the piston will break the equilibrium state and move up. On the contrary, when the servo tube moves down due to the elastic force of the spring, the pressure difference reduces and the piston will move down. So the piston movement can be driven by the lifting, maintaining and declining of the servo tube to move the control rod.

One critical characteristic of SHCM is the self-lock function in the balanced state. The position of the servo tube and the piston force is a one-to-one relationship, when the piston is balanced, an increase in the inlet pressure can cause a larger *F*, namely $F - G + F_{\Delta} > 0$. So the piston rises, leading to an increase of δ and a decrease of the resistance coefficient, the piston will set up a new equilibrium and remain stationary after rising to a certain position. On the contrary, if the inlet pressure is decreased, namely $F - G + F_{\Delta} < 0$, the piston will set up a new equilibrium and remain stationary after declining to a certain position. The drive mechanism has a self-balancing function.

The other important characteristics are the simple structure and the low energy consumption which can optimize the control system. Firstly, the driving force of the mechanism is not the traction force of the servo tube, but the pressure difference on the piston. It is simple to achieve the goal of controlling the control rod by moving the servo tube. Moreover, the piston is both the actuator and the locator, and the servo tube tractor can maintain the position of the control rod due to its self-locking capacity when the power or pressure is lost. Furthermore, when the transmission belt is disengaged, the load drops to the bottom in two seconds, SHCM can thereby achieve the goal of reactor tripping. Finally, the drive mechanism does not require many external control valves, there by making operation more reliable.

Table 1 Design parameters of SHCM

Design parameters	Value
Load(kg)	50
Cylinder diameter(mm)	100
Piston rod diameter(mm)	30
Servo tube diameter(mm)	60
Temperature(K)	298
Inlet pressure(MPa)	0.1-1.05
Flow rate(t/h)	0.88-4.84

3 Experimental system

The experimental system is a closed fluid circuit composed of a pump, a water tank, the test section, two flow meters, two pressure sensors and a data acquisition system (Fig.3). It also contains certain auxiliary equipments such as the filter, control valve and so on. The system sample frequency is 100 Hz, the inlet pressure, outlet pressure and flow rate will be collected, and then the dynamic process of experimental system can be fully recorded.

When the experiment begins, the pump extracts water from the tank, most of the water flows back into the tank through the bypass, the rest of the water flows into the drive mechanism and then goes back to the tank. The servo tube is lifted by the tractor, at this time, the piston moves upwards due to the action of the fluid pressure, this is the lifting stage. On the contrary, when the servo tube moves down, the piston will fall down too due to the gravity of the control rod, this is the declining stage. The experimental operation has two methods: (I) the piston is fixed, we define δ=0 as the zero point, change δ through lifting the servo tube, and then record the data of the system with different δ. (II) the piston can be moved, and the system dynamic processes in different work stages can be recorded. At every measure point, the valve is controlled so as to increase the inlet pressure gradually across the experiment, the data is recorded continuously in a

stable pressure range and measured 3 times under each work pressure.

(a) Experimental set-up

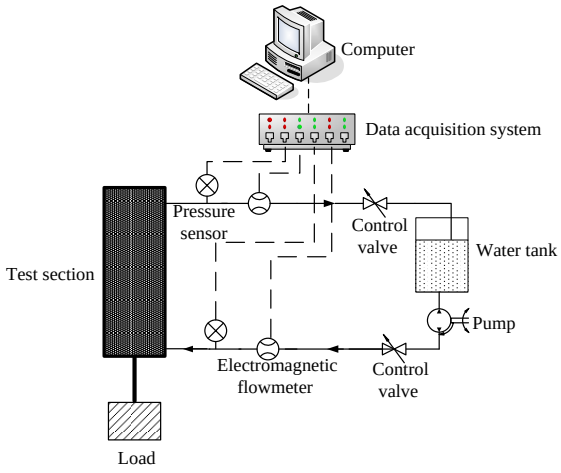

(b) Experiment circuit

Fig.3 Schematic diagram of experimental system.

When the experiment begins, the pump extracts water from the tank, most of the water flows back into the tank through the bypass, the rest of the water flows into the drive mechanism and then goes back to the tank. The servo tube is lifted by the tractor, at this time, the piston moves upwards due to the action of the fluid pressure, this is the lifting stage. On the contrary, when the servo tube moves down, the piston will fall down too due to the gravity of the control rod, this is the declining stage. The experimental operation has two methods: (I) the piston is fixed, we define $\delta=0$ as the zero point, change δ through lifting the servo tube, and then record the data of the system with different δ. (II) the piston can be moved, and the system dynamic processes in different work stages can be recorded. At every measure point, the valve is controlled so as to increase the inlet pressure gradually across the experiment, the data is recorded continuously in a stable pressure range and measured 3 times under each work pressure.

The main experimental equipment is introduced in Table 2. The pump provides a stable working pressure. The electromagnetic flowmeter and the pressure sensor measure the state parameters of the system. The DC servo motor hoists the servo tube, and the dynamometer measures the traction force. In addition, the displacement is obtained using the vernier caliper.

Table 2 Experimental equipment

Equipment Name	Type	Operating parameter	Error
Pump	2GC-5X4	Flow rate: 10 m^3/h	
Electromagnetic flowmeter	MSLD-15-1-0-0.4-E-Y-1-0	Output signal: 4~20mA Range: 0~6 m^3/h	1.5%
DC servo motor	DCL-MOIG	Output torque：16Nm	3%
Pressure sensor	WP401A-5G24EZ	Range: 0~3MPa Output signal: 4~20mA	0.5%
Dynamometer	LTZ-30	Range: 30~300N	2%
Vernier caliper	530-109	Range:0~300mm	2%

4 Simulation method used for the SHCM

Numerical simulations of flows in different conditions have been carried out widely in recent years. For a new design, no detailed analysis has been performed using computational fluid dynamics to predict the flow inside the SHCM. The purpose of numerical simulation is to verify the hydraulic performance and optimize the structure of the SHCM. One of the main issues of numerical simulation concerns the working characteristics of the servo tube.

4.1 Numerical solution methodology

The simulation of the fluid flow inside the cylinder was obtained using the FLUENT code in ANSYS workbench 12.0[6]. The code solves the 3D Navier-Stokes equations, discribed by a finite-volume second order upwind-differencing scheme. The convergence criterion for the normalized residual of an individual equation is set to be less than 10^{-6}. Steady-state solutions were obtained iteratively by the use of the predictor–corrector semi-implicit pressure linked equations (SIMPLE) algorithm[5][7].

4.2 Computational mesh and turbulence model

As Figure 4 shows, the volume inside the cylinder was discretized into an unstructured mesh with tetrahedral cells. Sensitivity analysis by changing node numbers was carried out, where the number of needed cells were taken between 500,000 and 1,000,000, and the comparison results of different case of mesh numbers showed that the case of total mesh is 850,000gave the more accurate one.

Different turbulence models such as the standard k-ε model, k-ω model and Reynolds Stress model were tested in this study. The results are compared in Figure 5. The simulation results are compared with experimental data. The flow rate difference between the standard k-ε model and the experimental data is the smallest, which indicates that the standard k-ε model is more accurate to describe the flow inside the mechanism. According to the fluid velocity, the temperature and the model complexity, the standard k-ε model was chosen for this study, and this was verified by the modeling comparison with experimental data.

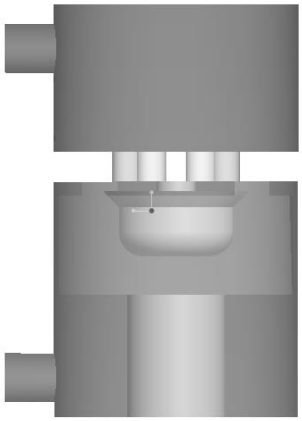

(a) 3D model of SHCM

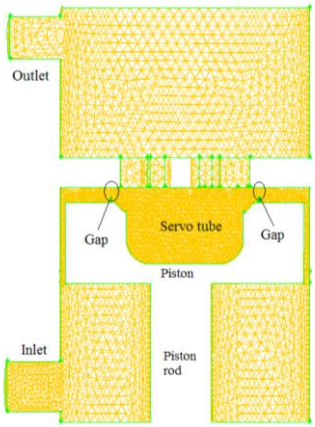

(b) mesh model

Fig.4 Schematic diagram of SHCM.

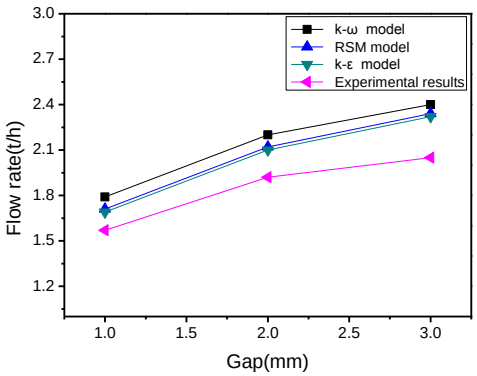

Fig.5 Comparison of the calculation results of different turbulence models.

4.3 Boundary conditions

All the simulations were performed with the following boundary conditions, chosen by consulting the relevant literature, including He *et al* (2007), Li *et al* (2010) and Wang *et al* (2004)[3][6][7]:

(1) The inlet pressures are 0.1MPa and 0.3MPa,

chosen with the aim to compare with the experimental results.

(2) Initial values of k and epsilon are assigned according to a 5% turbulence intensity level which is calculated from the average of the experiment results.

(3) The operating pressure is 101325 Pa, and the fluid is directly ejected outside, so the outlet gauge pressure is zero.

(4) No-slip conditions are assumed at the solid walls, and the wall function is used to deal with the wall boundary conditions.

5 Results and discussion

5.1 Steady state hydraulic characteristics of SHCM

Analysis of the hydraulic characteristics of the SHCM in steady state attempts to discover the key factors of the design, and then optimize the structure, and finally to prove the viability of the SHCM. The hydraulic behavior of the SHCM in operational conditions is characterized by the local pressure difference produced by the servo tube. In turn, the resistance coefficient of the servo tube can be used to characterize the pressure difference.

The resistance coefficient is as follows:

$$\xi = \frac{2\Delta p}{\rho v^2} \qquad (5)$$

There are two aspects of the resistance coefficient which have to be addressed. The first question involves the influence of the servo tube diameter on the resistance coefficient. It is observed that the change of the resistance coefficient are similar with different diameters (See Fig.6(a)). When the gap is less than 1.0 mm, the resistance coefficient increases quickly with the decrease of the gap. With the gap increasing, the resistance coefficient decreases slowly. Under the same gap, the greater the servo tube diameter is, the smaller the resistance coefficient is.

In this design, considering the accident protection function, the drive mechanism should be able to accelerate the control rod to a certain speed in a given time. The ultimate aim is to shorten the action time of the accident, therefore, a smaller resistance coefficient has been chosen. The servo tube diameter is 60mm.

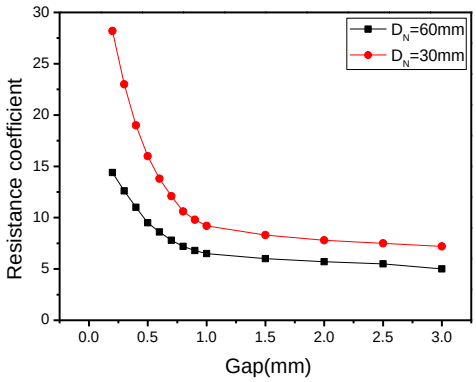

(a) Comparison of simulation results

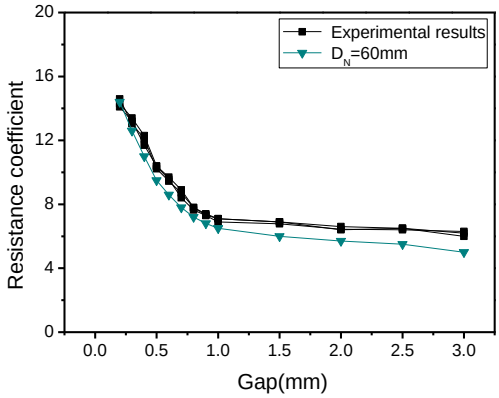

(b) Comparison between simulation results and experimental results

Fig.6 Resistance coefficient with different gap of variable throttle orifice.

The second problem relates to analyzing the results of the simulation and the experiment (See Fig.6(b)). The analysis shows that the simulation results agree well with the experimental results when the gap is less than 1.0mm (the servo tube diameters are all 60mm both in the simulation and the experiment). However, there is a small difference between them. This difference arises in part from the simplifications of the simulation model which causes the frictional resistance coefficient to be reduced. In addition, the pipe pressure losses are not considered in the calculation. The data reported here suggests that it is feasible for the performance characteristics of the SHCM to be studied by numerical simulation.

The flow rate and the drive force of the piston were obtained from the simulation (See Fig.7-8).

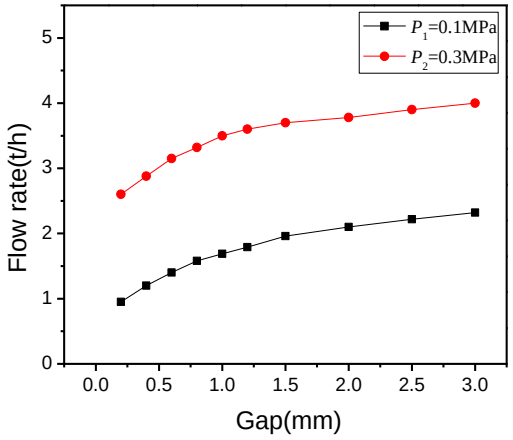

Fig.7 Flow rate results of simulation.

The results indicate that the flow rate increases with gap enlargement, while the drive force decreases rapidly when the gap is less than 1.2mm. The change rate of these parameters decreases slowly when the gap increases. If the gap is varied within the range of 0.5mm, the drive force of the piston will change dramatically, this means the piston will be moved or stopped. It can be inferred that when the piston is in an equilibrium state, if the servo tube is moved within 0.5mm, the motion state of the piston will be changed, so as to move the control cod. The response time of the SHCM is short, and the sensitivity is good. Furthermore, the working gap decreases gradually with the increase of the inlet pressure .

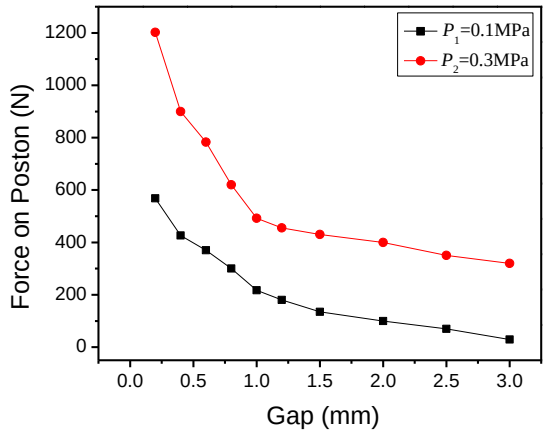

Fig.8 Change curves of drive force on piston.

It was therefore demonstrated that the SHCM can provide enough driving force to drive the control rod. In addition, the servo tube directly influences the working performance of the drive mechanism, consequently, it is the core component.

5.2 Dynamic experimental performance of SHCM

Experimental analysis of the SHCM aims at proving its reliability, testing the working performance and revealing the motion laws of the SHCM.

5.2.1 Force analysis of servo tube

When the drive mechanism is at different working conditions, the traction forces of the servo tube are also different. The experimental results of the traction forces are shown in Figure 9. Through analysis of the data it can be seen that the traction forces are larger in the starting stage and the braking stage, especially when the inlet pressure is 0.15 MPa. The traction forces are smaller in the lifting and declining stages. As the working pressure increases to 0.25 MPa, there is a step change of the traction force where it reduces quickly. When the working pressure is greater than 0.55 MPa, the traction force is almost stable. There is little traction difference between the starting stage and the braking stage, as well as the lifting stage and the declining stage. This is because the load force applied to the servo tube has been reduced significantly through liquid pressure transformation, so the traction forces of similar stages show little difference.

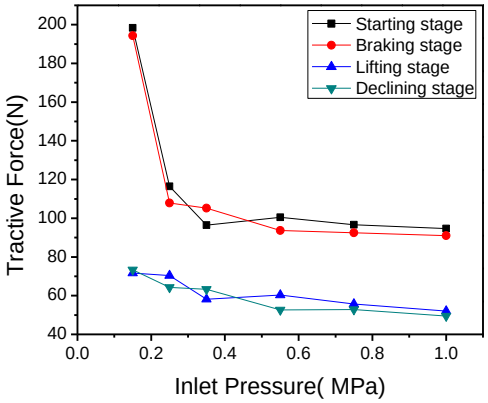

Fig.9 Changing curve of the traction force with different inlet pressures.

Traction force analysis aims to provide a basis for selecting a suitable motor. The motor output power is as follows:

$$P_w = \frac{F_t \cdot V_s}{\eta_t} \tag{6}$$

The maximal traction force in the experiments is 202N, the maximal moving velocity of the servo tube is 10 mm/s. The servo tube tractor is a combination device, including a coiling block, a worm-gear reducer and two couplings. The individual mechanical efficiency of these parts were taken from Ref.(8) and the overall mechanical efficiency of the servo tube tractor η_t was calculated as 0.66. The maximum output power is 9.18 W calculated from Eq.(6).

It indicates that the requirement of the motor power is very low. However, a slightly larger motor should be chosen in order to ensure safety in practice.

5.2.2 Transient Flow Characteristics

The dynamic processes of the system in different working processes were identified (See Fig.10). It is clear that the change trends are similar under different inlet pressures, however, the values are different. There is a lift delay process in lifting stage, because the servo tube has moved to a certain position to produce enough pressure difference. Furthermore, the delay time decreases with the increase of the inlet pressure, while the flow rate increases too. In addition, the lifting-flow rate is equal to the holding-flow rate under the same inlet pressure. This indicates that the servo tube and the piston are relatively static in the lifting process, the gap is constant, the flow rate does not change at this moment.

When the inlet pressure is 0.15 MPa, the drive mechanism can lift the 50 kg load, the maximum flow rate is only 2.02 t/h, so the power requirement of the pump is low. Moreover, when the reactor is running stably, the pump can be turned off because of the self-locking function of the servo tube tractor.

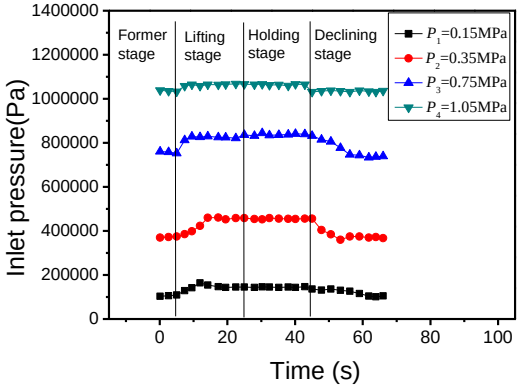

(a) Inlet pressure change process

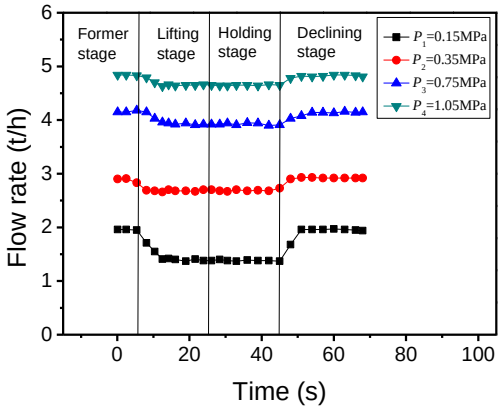

(b) Flow rate change process

Fig.10 Dynamic process of inlet pressures and flow rates.

5.2.3 Anti-disturbance characteristics

The experimental results of the resistance coefficient under different inlet pressure were obtained (See Fig.11). The dynamic curves all have similar form, with the resistance coefficient stable during the early stages. Then when the servo tube is lifted at 7.5 s, the resistance coefficient firstly increases, then trends towards a constant. The resistance coefficient decreases with the increase of the inlet pressure. However, there are differences when the inlet pressures are 0.15MPa and 0.35MPa. The resistance coefficient achieves a peak and then decreases to a constant, as shown at points a and b. It can be proved that the peaks are caused by the transient start-up force (See Fig.9). When the inlet pressure is lower, the transient start-up force is larger. With the inlet pressure increasing, the piston drive force is large enough to overcome it. At the same time, the gap is bigger, so the resistance coefficient is smaller (See Fig.6), for this reason the peak is unapparent in the other three curves.

The results also indicate that the small anti-disturbance capacity of the mechanism is good. Because the resistance coefficient changes in a small range during the holding stage, this suggests that the inlet pressure is not stable, but the load does not shake at all.

Importantly we ask when the disturbance is large, if the SHCM can keep working stably? The result shown in Figure 12 indicates that when the inlet pressure changes in a large range, the load position changes within 1mm. It can be inferred that the piston will return to an equilibrium state within 1 mm because of its self-balancing function if there

are some disturbances which lead to break the initial equilibrium state.

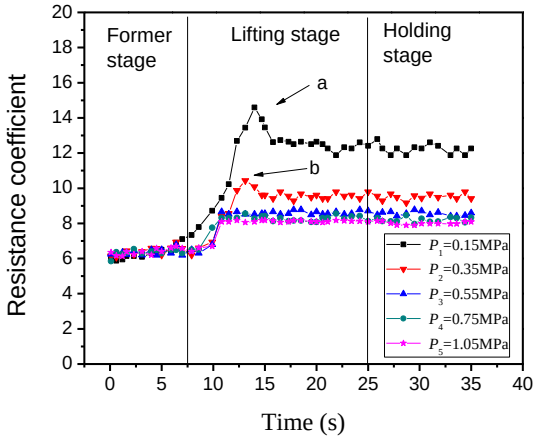

Fig.11 Resistance coefficient in working processes.

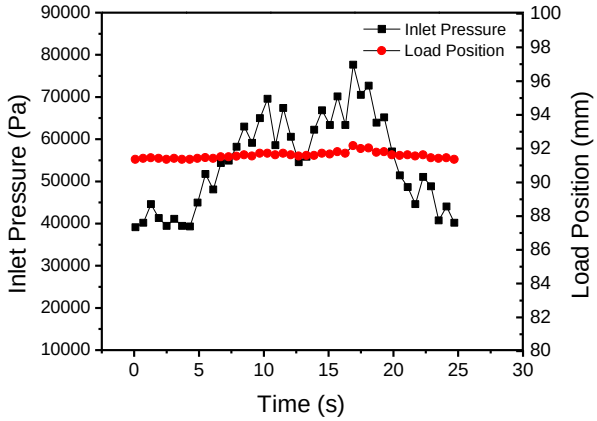

Fig.12 Load position in changing inlet pressures.

It is also proved that the SHCM can maintain stability and work properly under changing conditions. The limit of the working pressure and the flow rates of the SHCM are wide. Thus we can infer that its adaptability is good. If the inlet pressure increases suddenly, the fluid pressure on the piston bottom instantly increases, thus the piston will move upwards, so the gap will increases instantly which leads to a decrease in the pressure difference of the piston, then the piston will restore balance again. This implies that a rod ejection accident would not happen.

5.2.4 Positioning accuracy analysis

When the worm-gear reducer in the servo tube tractor turns a circle, the servo tube displacement is 3.64 mm, the actual lifting and declining displacements of the load are obtained by experiment (See Fig.13).

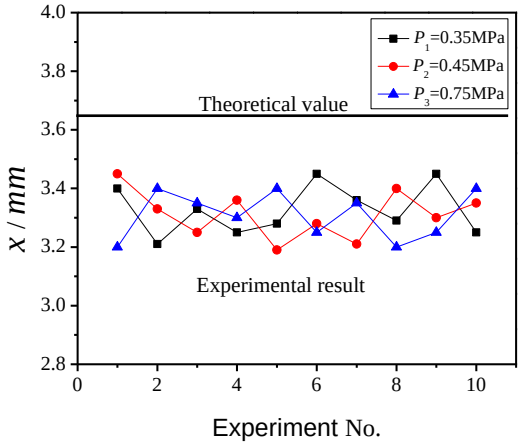

(a)Lifting stage

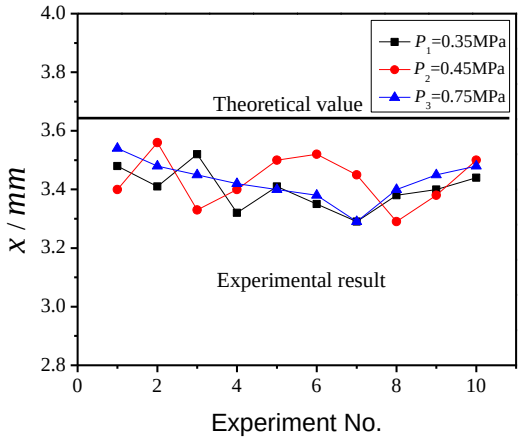

(b)Declining stage

Fig.13 Load displacement with different inlet pressures.

It can be seen that the displacement of the load compared with the servo tube is lagging. The displacement of the lifting stage is less than the declining stage, with average displacements of 3.31 mm and 3.42 mm respectively, and the difference to the theoretical value is less than 0.5mm, these results also proves that the simulation results are reasonable. Furthermore, the positioning accuracy does not change with the inlet pressure, a steady transformation can be realized in every working condition.

5.3 Comparison of SHCM and STCM

As a final element, the characters of two hydraulic control rod drive mechanisms are compared in Table 3.

Compared with STCM[9], the piston weight of SHCM is one-tenth of the piston weight of STCM, with the

servo tube volume is one-eighth of STCM. This means that the basic power requirement of the motor of SHCM is smaller than STCM because of the lighter piston. Furthermore, the transmission line is reduced by half, so the height of the drive mechanism will be reduced. Moreover, the positioning accuracy and the anti-disturbance capacity are improved, while the work pressure and the work flow change a little. The results of the comparison suggest that the performance of the SHCM is better than the STCM.

Table 3 Characteristics of two types of CRDM

Name	STCM	SHCM
Piston mass(kg)	16.5	1.5
Servo tube Diameter(mm)	36	60
Servo tube Length(mm)	900	40
Diameter of piston rod(mm)	80	30
Inlet pressure(MPa)	0.38	0.36
Flow rate(t/h)	2.02	2.4
Length of transmission line(mm)	1800	900
Location error	7%	5.5%
Anti-disturbance capacity	Small disturbance resistance	Strong disturbance resistance

6 Conclusions and summary

In this paper, a new type control rod drive mechanism has been designed, with good results obtained by the use of both simulation and experiment. The main conclusions obtained are as follows:

(1) The servo tube is the core component. The resistance coefficient and the driving force decreases with the increase of the gap of the variable throttle orifice, while the flow rate increases. The displacement of the servo tube changes within 0.5mm, the motion state of the piston can be changed.

(2) The piston just keeps the equilibrium position and can locate accurately under different pressure fluctuations, the main advantages of the SHCM including the anti-disturbance characteristic and the self-lock capacity are proved by the experiment.

(3) The experimental results show that the energy consumption of the SHCM is low, which indicates that the motor and pump requirements are easy to achieve.

The experiments under different work conditions have been carried out, the feasibility of the drive mechanism under normal working conditions is proved. It should be noted that the simulation model is built under steady-state conditions and the results are not fit for dynamic conditions of a nuclear reactor. The experiments were done under the condition of room temperature, the results will differ with the results under high temperature and high pressure conditions. Dynamic grid techniques are used to calculate the dynamic problem, an experimental system of adjustable temperature and pressure will be built. Despite its preliminary characteristics, this study has clearly indicated the feasibility and benefits of the SHCM.

List of acronyms

CFD	computational fluid dynamics
CRDM	control rod drive mechanism
HCRDS	hydraulic control rod driving system
N-S equations	Navier-Stokes equations
SHCM	servo-piston hydraulic control rod drive mechanism
STCM	servo-tube guided hydraulic control rod driving system

Nomenclatures

δ Gap of variable throttle orifice,(mm)

A Cylinder flow area, (mm^2)

A_g Circular channel flow area, (mm^2)

A_f Variable throttle orifice flow area, (mm^2)

A_0 Diversion hole flow area, (mm^2)

ρ_a Average density of piston ,(kg/m^3)

ρ_w Working medium density , (kg/m^3)
V Mean flow velocity, (m/s)
V_s Velocity of servo tube, (m/s)
F_t Traction of servo tube, (N)
P_w Power of motor, (W)
t Movement time, (s)
P_1 Pressure under the piston, (Pa)
P_2 Pressure above the piston, (Pa)
D_1 Drive cylinder diameter, (mm)
D_2 Piston rod diameter, (mm)
D_N Servo tube diameter, (mm)
η_t Overall efficiency of servo tube tractor
ξ Resistance coefficient

References

[1] YAN Changqi: Engineering of Nuclear Reactors, pp. 110-113, Harbin: Harbin Engineering University Press, (2004).

[2] ZHENG Yanhua, BO Hanliang, DONG Duo.: The study on the hydraulic control rod driving system in cyclical swing, Nuclear Engineering and Design, Vol.237, 2007: 100-106.

[3] HE Keyu, HAN Weishi.: Numerical Calculation for Flow Field of Servo-Tube Guided Hydraulic Control Rod Driving System, Nuclear power engineering, Vol.31, Number.4, 2010: 121-124.

[4] HAN Weishi.: Servo tube positioning fluid actuator. Application number: 200810209668.1, The Chinese invention patent, 2009.

[5] Issa, R.I.: Solution of the implicitly discretised fluid flow equations by operator-splitting, J. Comput. Phys, Vol.62, 1986: 40-65.

[6] LI Pengfei, XU Miny, WANG Feifei.: Proficient in CFD- Engineering simulation and Actual cases, pp. 162,321, Beijing: Posts and Telecom Press, (2010).

[7] WANG Jinhua, BO Hanliang, ZHENG Wenxiang, JIANG Shengyao.: Numerical Simulation for Three Dimensional Flow Field of the Step Cylinder in Hydraulic Control Rod Driving System, Atomic Energy Science and Technology, Vol.38, Number.1, 2004:54-58.

[8] ZHANG Chunyi, HAO Guangping, LIU Min.: Retarder design by example, pp. 9, China Machine Press, (2010).

[9] He Keyu.: Study on New-style Hydraulic Control Rod Driving System, Harbin Engineering University, (2009).